

THE STUDY OF THE AMPLITUDE PROBABILITY DISTRIBUTIONS OF ATMOSPHERIC RADIO NOISE

TAKETOSI NAKAI

I. Introduction

The measurements of atmospheric noise by statistical method have been made since 1957, and information of the cumulative amplitude probability distribution of the envelope voltage of atmospheric noise has been obtained in the range of long- and medium-frequency, that is, the character of diurnal- and seasonal-change of the amplitude probability distributions at 50 and 100 kc, the effects of frequency on the character of the amplitude probability distributions have been investigated. As a result of a series of measurements of atmospheric noise, the questions arise as to how the amplitude probability distributions are to be interpreted and how various forms of the amplitude probability distributions are related to the characters of atmospheric noise and the receiver response and so on. But the measured amplitude probability distributions are dependent on so many factors, that is, the geo-graphical area of active storms, the noise structures of ground discharge and cloud discharge, the character of propagation of electromagnetic waves, the distance of propagation, and the receiver response and so on, and related factors are so complex that complete and precise data can not be used. Then we will assume that a statistical structure of atmospheric noise arriving at the antenna of the receiver and the receiver response, in order to derive the calculated amplitude probability distribution of the envelope voltage at the output of the receiver. The calculated amplitude probability distributions showed various forms dependent on the noise conditions, that is, density and strength in the assumed atmospheric noise. The comparison between the calculated- and the measured-amplitude probability distributions showed interesting fits in the frequency range of 50 kc to 500 kc. The theory used in deriving the amplitude probability distributions and the results obtained will be shown in detail and some examples of fitting between the calculated- and the measured amplitude probability distributions will be shown in this paper.

II. The theory of deriving the amplitude probability distribution

It is necessary to assume the character of atmospheric noise arriving at the antenna of the receiver to evaluate the amplitude probability distribution of the envelope voltage of atmospheric noise. Here, we will be able to utilize the facts that distributions of peak amplitude of atmospheric noise have been measured by some students.⁽¹⁾ Let us now assume, on the basis of the results of observations referred to, that atmospheric noise consists of a series of pulses which are waves of constant frequency modulated by a rectangular wave form of constant duration

and that the distribution of peak amplitude of pulses may be expressed by a log-normal distribution. Then the amplitude probability distribution of the envelope voltage of atmospheric noise at the output of the receiver may be derived as the sum of two sets of envelope voltages dependent on the receiver response given later, in which the one is due to the thermal noise and the other due to atmospheric noise. Related factors will be described in turn in the following.

2.1 Rayleigh-distribution

The set noise is expressed at the output of the receiver by the Rayleigh-distribution, that is,

$$P_R(v) = \frac{v}{\psi_0} \exp(-v^2/2\psi_0) \quad (1)$$

the cumulative probability is given

$$Q_R(v) = \frac{1}{\psi_0} \int_v^{\infty} v \exp(-v^2/2\psi_0) dv = \exp(-v^2/2\psi_0) \quad (2)$$

where v is the instantaneous envelope voltage, and ψ_0 is the mean square voltage.

2.2 Amplitude probability distribution of atmospheric noise

When a series of pulses are applied to the input of the amplifier, in which a pulse gives rise to a standard form of envelope voltage at the output of the receiver, and the distributions of peak voltages of pulses are given, and a series of envelope voltages are separated and do not interfere with each other, the required amplitude probability distribution may be evaluated by the following integral⁽²⁾

$$Q_A(v) = \int_v^{\infty} P(V) \cdot W(X) dV \quad (3)$$

where $P(V)dV$ = no. of pulses whose peak lie in the voltage range V to $V+dV$

$W(X)$ = width of the envelope voltage appearing at the output for the pulse of peak voltage V , at the threshold v

$$X = \frac{v}{V}$$

2.3 The receiver response

The component pulse in atmospheric noise is assumed to be the carrier of constant frequency modulated by a rectangular form and so it is expressed in the following manner,

$$e = e^{j\omega t} [1 - e^{j\omega(t-T)}] \quad (4)$$

where $\omega = 2\pi f$

T is the duration of the rectangular form and f is the measured frequency of atmospheric noise. And let us consider the receiver to be made of two stages of amplifiers, each with a single resonance circuit in the plate circuit as the load impedance. Then the transient response is expressed by the well known equation

$$F(Z) = 1 - e^{-Z} - Ze^{-Z} \quad (5)$$

when the carrier frequency is equal to the resonance frequency of the circuit. And when the 3-db bandwidth in the receiver is designated as f_b , Z is given by the well known relation

$$Z = 4.881 f_b t \quad (6)$$

Now, let us take a quantity proportional to the bandwidth f_b for the duration of the component pulse in atmospheric noise, that is, $Z=0.5$, or $Z=1.5$. Then, the response of the circuit for the carrier modulated by the rectangular form of duration, $Z=0.5$, or $Z=1.5$ could be evaluated on the basis of the equation(5).

When the pulse rate at the antenna is small, $W(x)$ could be evaluated for the specified pulse rate from the response curve for the component pulse of duration $Z=0.5$, or $Z=1.5$ respectively.

2.4 Peak voltage distribution

On the basis of assumptions of atmospheric noise, the peak voltage distribution of pulses may be written as;

$$P(v) = \frac{0.4343}{\sqrt{2\pi} \sigma v} \exp \left\{ -\frac{(\log v - \log m)^2}{2\sigma^2} \right\} \quad (7)$$

where v = peak voltage of pulse

m = peak voltage which the pulse exceeds by 50% of the sum of the durations of all the pulses

σ = the standard deviation of the logarithm of the pulse peak voltage about the mean.

2.5 $Q_A(v)$

The required amplitude probability distribution for pure atmospheric noise assumed at the antenna, $Q_A(v)$ indicated in equation (3), could be evaluated by using $P(v)$ given in equation (7) and $W(X)$ derived as described in section 2.3.

2.6 The superposition of the set noise and the atmospheric noise at the output of the receiver

The measured amplitude probability distributions of the instantaneous envelope voltage of atmospheric noise may be the sum of two sets of envelope voltages in which one is due to the thermal noise of the receiver and the other is due to the pure atmospheric noise. Then, it is necessary to consider the probability density of the two sets of envelope voltages in the time region where the pure atmospheric noise and the thermal noise exist simultaneously. The probability density may be written approximately as ⁽³⁾

$$P_{R+A}(v) = \int_0^v P_R(W) P_A(v-W) dW \quad (8)$$

where $P_R(v)$ is the probability density function given in eqn. (1), and $P_A(v)$ may be obtained by the differentiation of $Q_A(v)$, eqn. (3) with respect to v and it is necessary to resort the numerical calculations of the integral. eqn. (3), and of the differentiation of $Q_A(v)$ with respect to v .

Now, the required amplitude probability distribution may be written as

$$Q_I(v) = P_1 \int_v^\infty P_R(v) dv + P_2 \int_v^\infty P_{R+A}(v)_n dv \quad (9)$$

when the time region in which only the thermal noise exists and the time region in which the thermal noise and the atmospheric noise exist simultaneously, are expressed respectively by $P_1\%$ and $P_2\%$ of all the noise process. The integra. in the first term corresponds to the contribution of the thermal noise and the second integral corresponds to that of the sum of the thermal noise and the atmospheric noise. Here, some explanation must be given to the derivation of $P_{R+A}(v)_n$. Each of these functions shows the probability density of the sum of two envelope voltages and is given as

$$\left. \begin{aligned} P_{R+A}(v)_1 &= \int_0^v P_R(W)P_A(v-W)_1 dW \\ P_{R+A}(v)_2 &= \int_0^v P_R(W)P_A(v-W)_2 dW \\ \dots\dots\dots \\ P_{R+A}(v)_n &= \int_0^v P_R(W)P_A(v-W)_n dW \end{aligned} \right\} \quad (10)$$

where each of $P_A(v)_1, P_A(v)_2, P_A(v)_3, \dots, P_A(v)_n$, takes the same form of the probability density function of the envelope voltage expressed in logarithmic-scale and the same value of probability density corresponds to the envelope voltage separated at the step of 8 db for $P_A(v)_1, P_A(v)_2, \dots, P_A(v)_n$ in turn. This way of thinking corresponds to the case where the source distance varies while the assumed property of atmospheric noise remains constant.

2.7 Two systems of atmospheric noise

Thus far it has been considered that only one system of atmospheric noise exists and adds to the thermal noise of the receiver, and it has been shown that the amplitude probability distribution of the envelope voltage of atmospheric noise at the output of the receiver may be expressed as in eqn. (9). Further, it could be considered that two or more systems of atmospheric noise exist and add to the thermal noise of the receiver. Let us now assume that two systems of atmospheric noise exist, each with the same properties of pulse duration and pulse amplitude distribution as has been assumed before. Crudely speaking, one system of atmospheric noise may be considered to be propagated from sources in a short distance and the other may be considered to be from sources in a long distance. To simplify the required evaluation, let us consider that two systems of atmospheric noise do not have in common the time region of all the noise processes, each having its independent part of all the noise processes. When the time regions in which the two systems of atmospheric noise add to the thermal noise, are expressed by $P_1\%$ and $P_2\%$ respectively, the required amplitude probability distribution may be written as

$$Q_{\parallel}(v) = P_1 \int_v^{\infty} P_{R+A}(v)_n dv + P_2 \int_v^{\infty} P_{R+A}(v)_m dv \quad n < m \quad (11)$$

where the first term and the second may be considered to be the contribution respectively from the long-distance-sources and the short-distance-sources. In succession to the thinking described in the preceding section, various combinations of two systems of atmospheric noise may be considered, that is,

$$Q_{\parallel}(v) = P_1 \int_v^{\infty} P_{R+A}(v)_1 dv + P_2 \int_v^{\infty} P_{R+A}(v)_m dv \quad m = 2, 3, \dots \quad (12-1)$$

$$Q_{\parallel}(v) = P_1 \int_v^{\infty} P_{R+A}(v)_2 dv + P_2 \int_v^{\infty} P_{R+A}(v)_m dv \quad m = 3, 4, \dots \quad (12-2)$$

These relations represent the case in which the ratio of strength between the two systems of atmospheric noise is the multiple of 8 db, but this ratio of strength may be considered to take more subdivided values.

Here, let us add some experimental considerations in deriving the amplitude probability distribution, that is, let it be that the first integral is replaced by the experimentally evaluated amplitude probability distribution, the log-normal distribution with standard deviation 5 db. The experimental evaluation was made about the amplitude probability distributions measured at frequency more than 200 kc, at hours of the lowest level of atmospheric noise of a day. Then the

required amplitude probability distribution may be written as

$$Q_{\text{III}}(v) = P_1 \int_v^\infty \frac{0.4343}{\sqrt{2\pi} \sigma v} \exp \left\{ -\frac{(\log v - \log m)^2}{2\sigma^2} \right\} dv + P_2 \int_v^\infty P_A(v) dv \quad (13)$$

III. The results of numerical evaluation

3.1 $W_1(X)$, $W_3(X)$

$W(X)$ was calculated in the manner as described in section 2.3 when the pulses arrive at the antenna at the rate of a pulse in the elapse time of $Z=10$. The results of numerical evaluation are shown, in figure 1, on a graph paper with the envelope voltage on a logarithm-scale and the percent of time on a normal-scale, where $W_1(X)$ and $W_3(X)$ indicate the results for the pulse duration of pulse $Z=0.5$ or $Z=1.5$ respectively. The difference of the duration of pulse results in the different maximums response at the output of the receiver, but $W_1(X)$ and $W_3(X)$ were fitted at the maximum response for comparison of the forms of the two, along the abscissa.

3.2 The $Q_A(v)$

The formula for deriving the amplitude probability distribution of the envelope voltage of atmospheric noise assumed is expressed by equation (3). Now, $Q_A(v)$ can be evaluated for the given logarithmic-normal distribution with the standard deviation 8 db and $W_1(X)$ or $W_3(X)$ shown in figure 1 in section 3.1. The results of evaluation were shown, in figure 2, on a

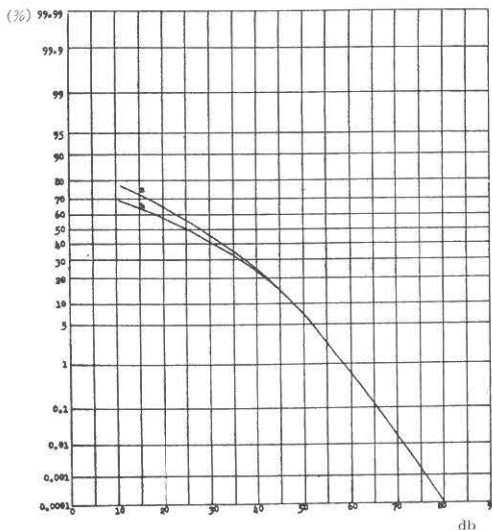


Fig. 2. The graphs of $Q_A(v)$. The signals a and b indicate $Q_A(v)$ evaluated for $Z=1.5$ or $Z=0.5$ respectively.

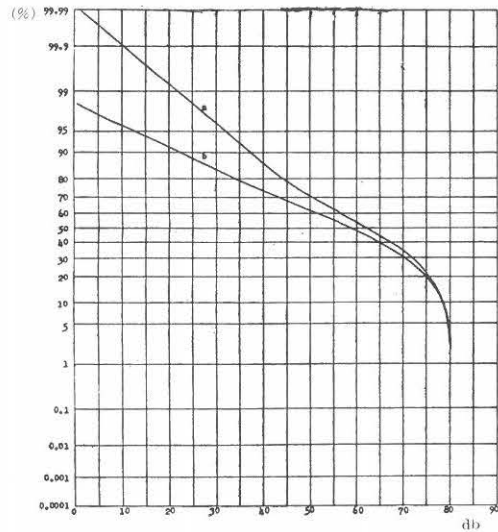


Fig. 1. The graphs of $W(X)$. a and b indicate $W_3(X)$ and $W_1(X)$ respectively.

graph paper with the threshold voltage on a logarithmic-scale and the fraction of time on a normal-scale, in which the two curves were fitted at the highest threshold voltage for comparison of the effects of the changes of pulse durations on the evaluated amplitude probability distributions. The trend of the two curves shows an approximate parallelism at higher range of threshold voltage and the change

of pulse duration affects the change of strength mainly with little effect on the form of the amplitude probability distribution. But the displacement of the two curves becomes appreciable in the lower range of threshold voltage.

3.3 The cumulative probability of the sum of the two kinds of noise

The probability densities given in eqns. (10) were evaluated for the given probability density $P_R(v)$ in eqn. (1) and a series of probability densities $P_A(v)_n$ as considered in section 2.6. Each of these probability densities $P_A(v)_n$'s was evaluated by graphical differentiation from the curves of their cumulative probability $Q_A(v)_n$'s each of which is expressed by the integral

$$\int_v^{\infty} P_A(V)_n dV.$$

These results of evaluation of the integrals of eqns. (10) were shown with the Rayleigh-distribution in figure 3 on a graph with the threshold voltage on a logarithmic-scale and the fraction of time on a normal-scale. The limit curve shows the Rayleigh-distribution and each of the real curves with the number of n showing

$$Q_{R+A}(v)_n = \int_n^{\infty} P_{A+R}(V)_n dV \quad (14)$$

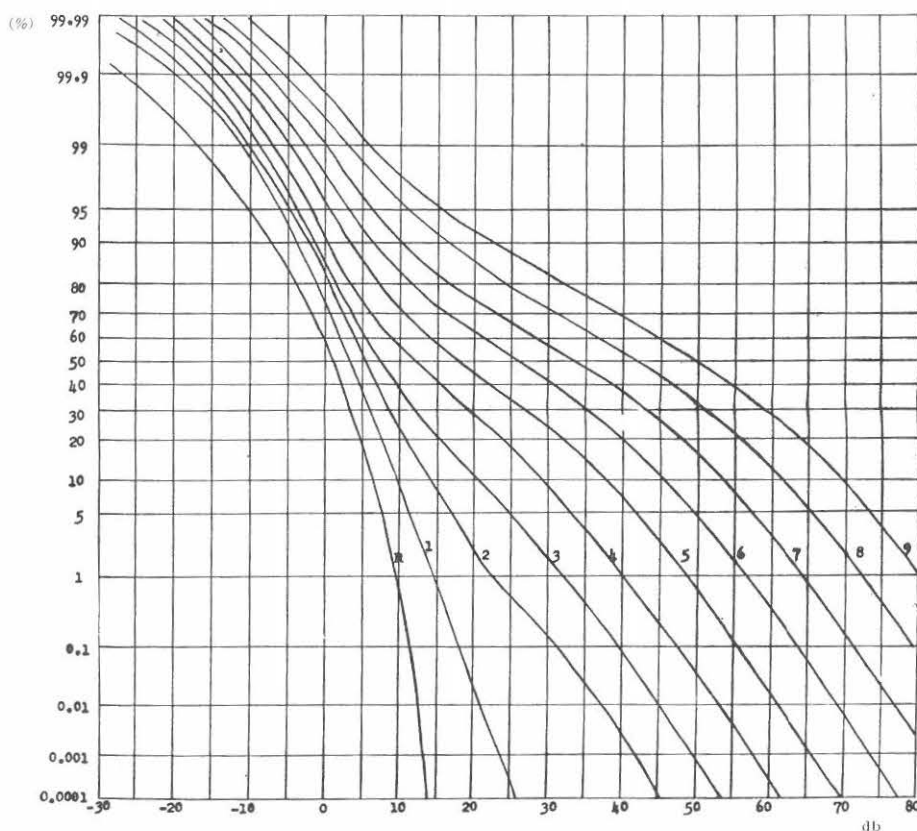


Fig. 3. The graphs of $Q_{A+R}(v)_n$. R: The Rayleigh distribution.
1: an arbitrary curve. 2: $Q_{A+R}(v)_2$

These integrals were carried by resorting numerical evaluation of the curves drawn by plottings of the calculated values of the probability densities $P_{R+A}(v)_n$ at the necessary points. The accuracy of the process of evaluation of the integrals in eqns. (10) and in eqn. (14) depends on the number of division points used in numerical integration and this was kept small enough to obtain the smoothly drawn curves.

3.4 The derived amplitude probability distribution

$Q_I(v)$'s were evaluated numerically under the variable changes of combinations of P_1 and P_2 , that is, $P_2=1/2, 1/4, 1/8, 1/16, 1/32, 1/64, 1/128, 1/256$. The

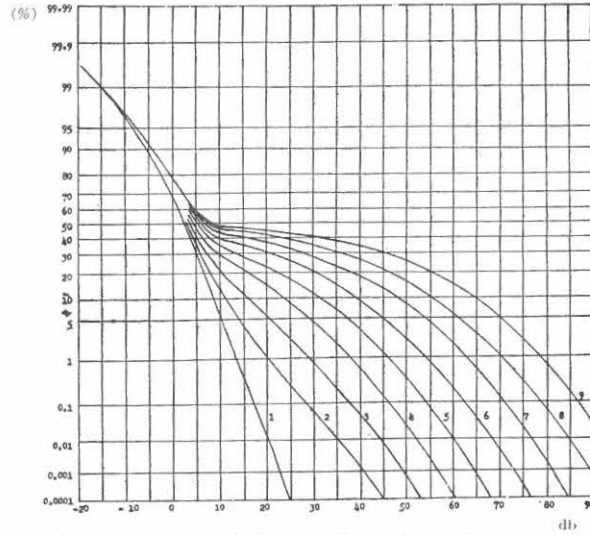


Fig. 4-1. The graphs of $Q_I(v)_n$ evaluated for the combination of $P_1=1/2, P_2=1/2$. $n: Q_I(v)_n$.

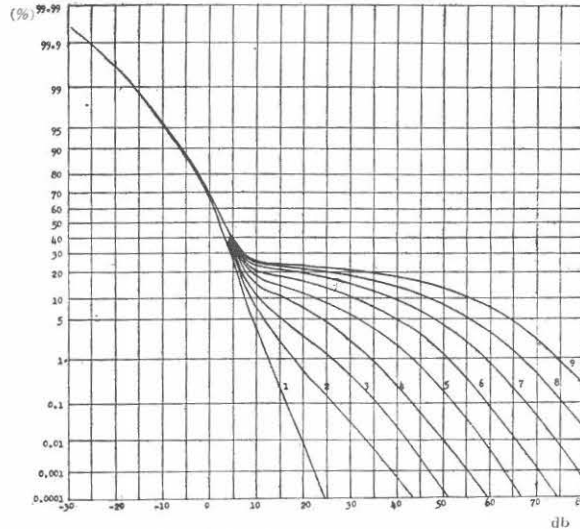


Fig. 4-2. The graphs of $Q_I(v)_n$ evaluated for the combination of $P_1=3/4, P_2=1/4$. $n: Q_I(v)_n$.

numerical results, for example, for the combinations $P_1=1/2$, $P_2=1/2$ and $P_1=3/4$, $P_2=1/4$ are shown in figure 4, on a graph with the fraction of time on a normal-scale and the threshold voltage on a logarithmic-scale. The figure n associated with each curve shows that it has been evaluated from the sum of the fixed thermal noise and atmospheric noise displaced by a step of 8 db in strength, as has been described in section 2.6.

$Q_{II}(v)$'s were evaluated numerically under different combinations specified as above. The numerical results are shown in figure 5 for the combinations $P_1=$

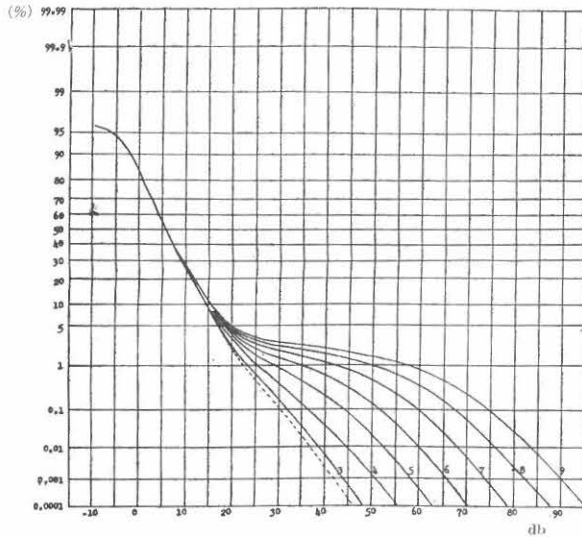


Fig. 5-1. The graphs of $Q_{II}(v)_n$ evaluated for the combination of $P_1=31/32$, $P_2=1/32$. $n: Q_{II}(v)_n$

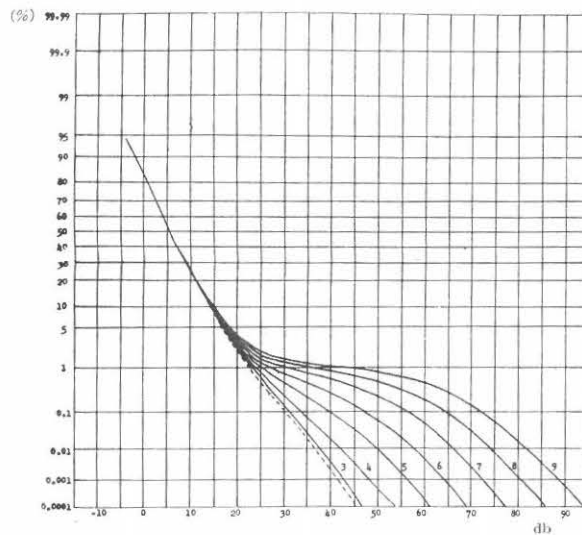


Fig. 5-2. The graphs of $Q_{II}(v)_n$ evaluated for the combination of $P_1=63/64$, $P_2=1/64$. $n: Q_{II}(v)_n$.

$31/32$, $P_2=1/32$ and $P_1=61/62$, $P_2=1/62$. The dashed curve shows the cumulative probability $Q_{R+A}(v)_2$, that is, it shows the amplitude probability distribution when the thermal noise and the atmospheric noise $P_A(v)_2$ superpose in all the noise processes. The real curves were evaluated from the equation (12-2) for different values of n . Similar examples of numerical evaluation of results of $Q_{III}(v)$ given by eqn. (13) are shown in figure 6 for the combinations of $P_1=7/8$, $P_2=1/8$ and $P_1=15/16$, $P_2=1/16$.

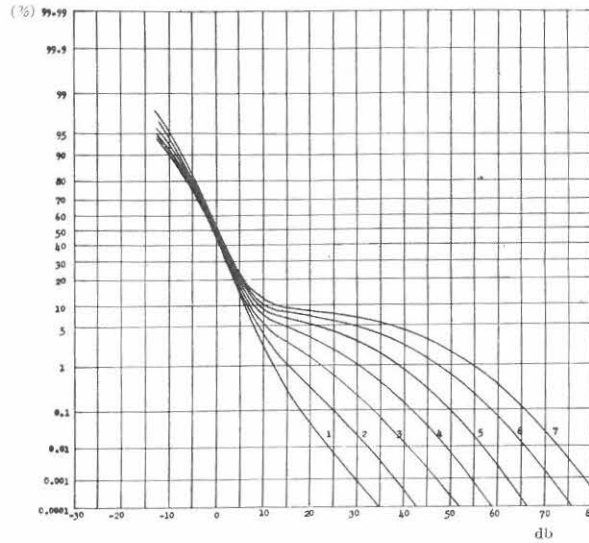


Fig. 6-1. The graphs of $Q_{III}(v)_n$ evaluated for the combination of $P_1=7/8$, $P_2=1/8$. $n: Q_{III}(v)_n$

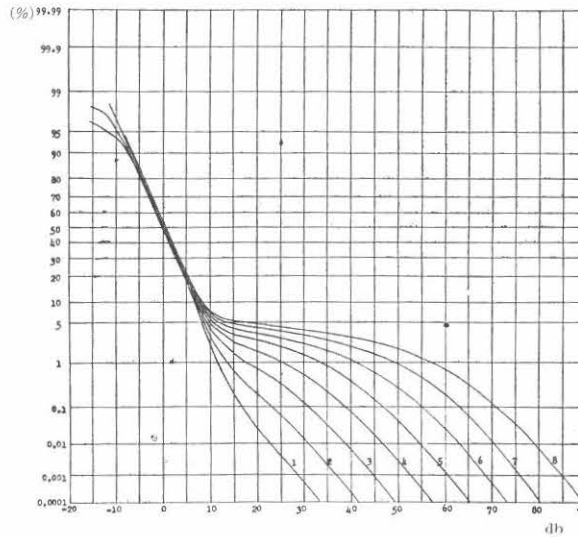


Fig. 6-2. The graphs of $Q_{III}(v)_n$ evaluated for the combination of $P_1=15/16$, $P_2=1/16$. $n: Q_{III}(v)_n$

IV. Comparison between the results observed and the results evaluated

4.1 The measured amplitude probability distributions at various frequencies

The amplitude probability distributions of atmospheric noise were measured in Toyokawa, during a week in August, 1959. The measurements were made every two hours in day time at several frequencies ranging from 50 to 500 kc. The amplitude probability distributions were successively made from a frequency to another frequency and a cycle of measurements took about 40 to 50 minutes. Conditions at the sources of atmospheric noise may be considered to have been roughly stationary, but considerable changes of atmospheric noise level were noted in the course of a cycle of measurements for some cases of measured amplitude probability distributions. The system of measuring apparatus have been reported elsewhere^{(4), (5)} and is not given here, but it must be noted that a vertical antenna 9 m long was used, and a little improvement has been made in automatically recording.

The curves in figure 7 show the average amplitude probability distributions and the degrees of discrepancy around them for all the measured amplitude probability distributions in the period of measurement at frequencies of 50 kc, 200 kc, and 500 kc. The derivations of these curves are as follows, that is, by neglecting the changes of the absolute levels and displacing all the measured amplitude probability distributions at each frequency along the threshold voltage to fit at the threshold voltages for 80%, the average of the threshold voltages in db were evaluated for given values of the fraction of time. The central curves in figure 7 show the results of the process of evaluation at each frequency and the two curves on each side of the central curves show the boarder lines, inside of which three fourth of all the evaluated values exist while outside of which exists one fourth.

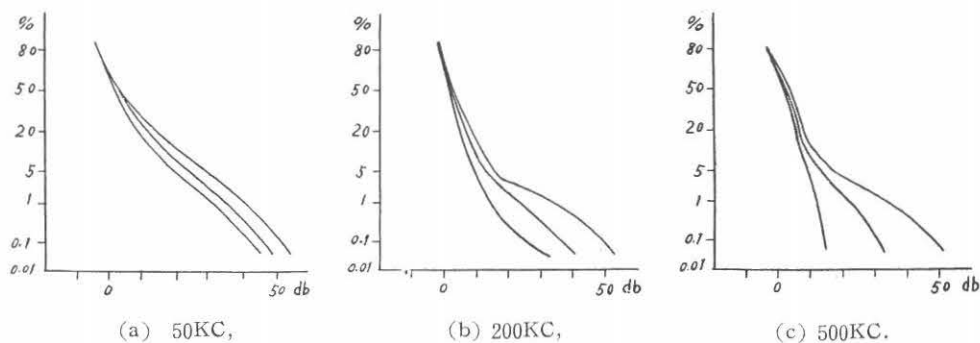


Fig. 7. The graphs showing the mean amplitude probability distributions and dispersion of the forms at different frequencies.

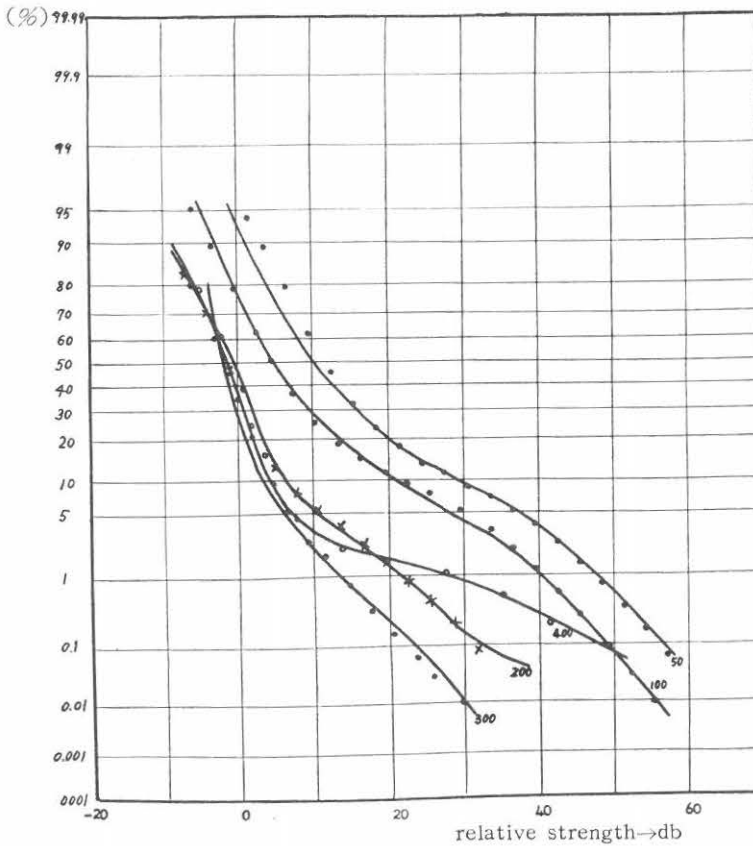
Comparison between the behaviors of the amplitude probability distributions at indicated frequencies in figure 7 shows that at a lower frequency the forms of the amplitude probability distributions display themselves more stationary and at a higher frequency they are more variable. This trend may be interpreted by considering that the effect of atmospheric noise from long distance sources is

more appreciable when compared to that of atmospheric noise from short distance sources and therefore the effect diminishes gradually towards higher frequencies.

4.2 The results between the measured- and measured- amplitude probability distributions

We have obtained three sets of evaluated amplitude probability distributions, that is, for $Q_I(v)$ in eqn. (9), $Q_{II}(v)$ in eqns. (12) and $Q_{III}(v)$, in eqn. (13). The measured amplitude probability distributions were examined regarding the conditions fitting to the evaluated amplitude probability distributions of these sets. The conditions depend on various combinations of P_1 and P_2 , and the level difference between two systems of atmospheric noise or between the thermal noise and a system of atmospheric noise to be added. Generally speaking, the results of comparison show that good fits were obtained between the amplitude probability distributions measured at 400 and 500 kc, and the amplitude probability distributions evaluated from $Q_I(v)$, and fair fits were obtained between the amplitude probability distributions at 50 kc and that evaluated from $Q_{II}(v)$.

Fig. 8-1. The comparison between the evaluated- and measured- amplitude probability distributions of atmospherics at several frequencies.



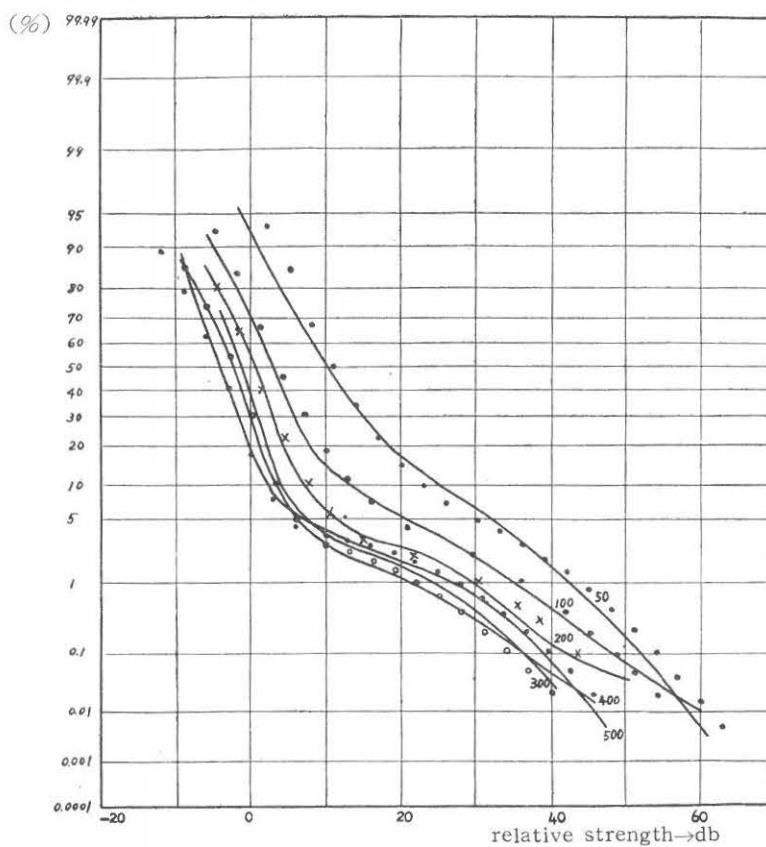
Some examples are shown in figure 7. The measured amplitude probability distributions at several frequencies were drawn on a graph with the threshold voltage on a logarithmic scale and the fraction of time on a normal scale, and the signals '•' and '×' show the traces of the evaluated amplitude probability distributions. The situations of fits are shown in the following tables.

One sample was measured at 12h on 5th August, 1959 and is shown in fig. 7-1.

TABLE 1.

frequency (KC)	density (P_2)	relative field strength(db)	kind of the calculated curve
50	1/4	0	$Q_{II}(v)$
100	1/4	- 6.8	$Q_{II}(v)$
200	1/4	-24.8	$Q_I(v)$
300	1/4	-32.8	$Q_I(v)$
400	1/4	- 2.8	$Q_I(v)$

Fig. 8-2. The comparison between the evaluated- and measured- amplitude probability distributions of atmospherics at several frequencies.



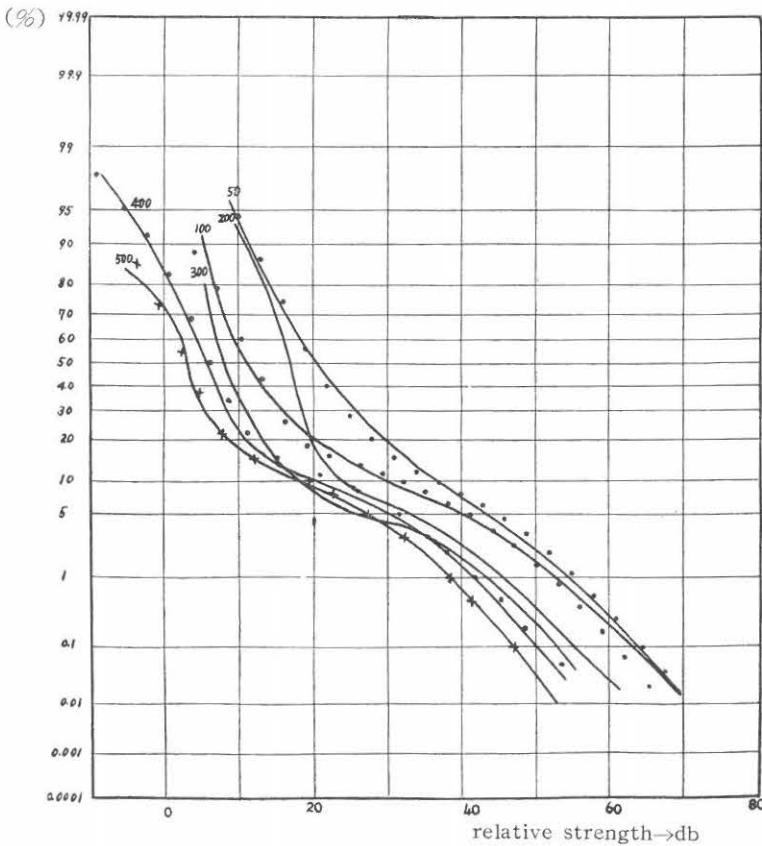
The results show that the density of pulses is 1/4 in the range of frequency of 50 kc to 300 kc, but it is 1/32 at the frequency of 400 kc with a considerable enhancement of level. It shows that the conditions of the sources of atmospherics happened to change at the measurement at 400 kc in a cycle of course.

The second sample was measured at 14h on 6th August, 1959 and is shown in fig. 7-2.

TABLE 2.

frequency (KC)	density (P_2)	relative field strength(db)	kind of the calculated curve
50	1/8	0	$Q_{II}(v)$
100	1/16	- 3.5	$Q_{II}(v)$
200	1/16	- 9	$Q_{II}(v)$
400	1/16	-17	$Q_I(v)$
500	1/16	-11.5	$Q_I(v)$

Fig. 8-3. The comparison between the evaluated- and measured- amplitude probability distributions of atmospherics at several frequencies.



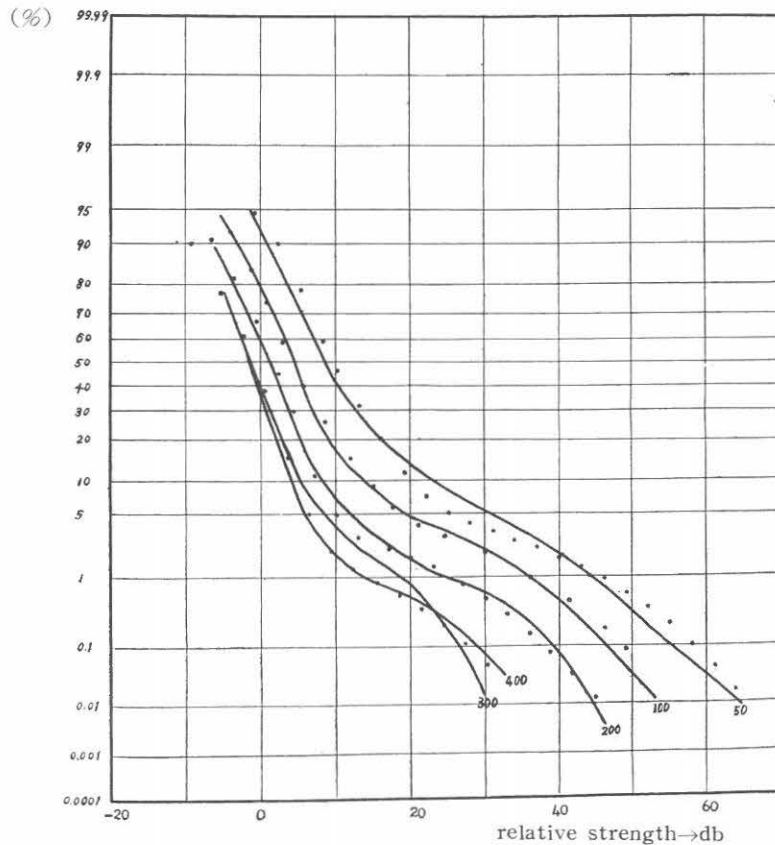
The density of the pulses is $1/16$ at all the measured frequencies except 50 kc, in which case it is $1/8$. This may be interpreted that the conditions of the sources of atmospherics changed after the measurements at 50 kc had been finished, because the measurements were made, beginning at 50 kc and going up towards higher frequencies.

The third sample was measured at 16h on 6th August, 1959 and is shown in figure 7-3.

TABLE 3.

frequency (KC)	density (P_2)	relative field strength(db)	kind of the calculated curve
50	$1/4$	0	$Q_{II}(v)$
100	$1/4$	-4	$Q_{II}(v)$
400	$1/4$	-13	$Q_I(v)$
500	$1/4$	-17	$Q_I(v)$

Fig. 8-4. The comparison between the evaluated- and measured- amplitude probability distributions of atmospherics at several frequencies.



The level difference between different frequencies is diminished and it may be interpreted as the reflection of the frequency spectrum of amplitude at the source of atmospherics, due to the short distance of propagation. The parts of the amplitude probability distributions at a high threshold voltage display similar curvatures to those of the frequencies indicated in Table III, and it may be considered that the density of pulses is 1/4. The deformation of the amplitude probability distribution at 200 kc may be considered to have been affected by an interfering noise.

The fourth sample was measured at 12h on 7th August, 1959 and is shown in figure 7-4.

TABLE 4.

frequency (KC)	density (P_2)	relative field strength(db)	kind of calculated curve
50	1/16	+ 8	$Q_{II}(v)$
100	1/16	- 1.5	$Q_{II}(v)$
200	1/16	-12.5	$Q_{II}(v)$
400	1/16	-23	$Q_I(v)$

The amplitude probability distribution at 300 kc displays a rapid decrease of the measured probability against threshold voltage, and no fair fit was obtained with the evaluated amplitude probability distribution.

4.3 The effect of pulse duration

The derived amplitude probability distributions are on a basis of the assumed atmospheric noise in which the pulse duration was given by $Z=1.5$. It must be discussed how the change of pulse duration affects on the amplitude probability distributions. With view to the discussion in section 3. 2, the change of pulse duration may have small effect on the deformation of the amplitude probability distributions, but it does result in an apparent change of strength of atmospheric noise, in which the duration of pulse remains constant. Considerable change of pulse duration has not been considered in this paper.

V. Conclusion

We have assumed the statistical structure of atmospheric noise arriving at the antenna and the receiver response, and derived the amplitude probability distributions. The comparison between the evaluated- and measured-amplitude probability distributions showed approximate fits. Here some conclusions are stated as follows.,

1. The assumed distribution of peak voltage may be considered to be appropriate, but it may not always be necessitated.
2. The pulse duration of atmospheric noise was considered to be constant, but a change of the pulse duration can be transformed into a change of the peak voltage of the pulse having the same pulse duration.
3. We considered the case where two systems of atmospheric noise existed in separated time regions and not superposing each other. This treatment may be approximate.
4. The receiver response was considered of the two stages of the simple

resonance circuit. For the given bandwidth, the effects of different constitution of circuits was not considered. For a given constitution of circuits, the effects could be evaluated.

5. The amplitude probability distributions measured at a higher frequency, for example, at 400 kc and 500 kc, can be considered to be the sum of the thermal noise and a system of atmospheric noise. On the other hand, the amplitude probability distribution measured at 50 kc must be interpreted to be the effects of two systems of atmospheric noise. This interpretation agrees with the experimental results in the frequency range of 50 kc to 500 kc.

6. Examples of fits between the measured- and evaluated amplitude probability distributions show that the parts of the amplitude probability distributions at a high threshold voltage are mainly affected by the input of the short distance atmospheric noise of the same density in the measured frequency range. And it may be considered that the field strength or the mean of peak voltages of pulses in a short distance atmospheric noise at the antenna is the ratios of the threshold voltages at a low percent of probability, for example, 0.1% in the measured frequency range. But this statement assumes that the pulse durations are the same for the receiver with the same bandwidth at different frequencies. When the pulse durations change in the measured frequencies, the ratio of the threshold voltages for the probability of 0.1% must show the apparent relative field strength at different frequencies, because the changes of the pulse durations are transformed into the changes of field strength.

7. Further research is hoped for of fits between the measured- and the evaluated-amplitude probability distributions in many cases.

VI. Acknowledgement

The author wishes to thank Prof. A. Kimpara, Director of the Research Institute of Atmospheric, for his continual encouragement and interests in these problems.

He also wishes to thank Mr. Y. Suzuki for his valuable assistance in carrying out the observation and Miss. M. Ito for her valuable assistance in preparing this paper.

VII. References

- 1) F. Horner : J. A. T. P. Vol, 13, Dec., 1958
- 2) J. Harwood : I. E. E. Part B, No. 21, May., 1958
- 3) Holbrock, B. D., and Dixon, J. T., Bell system Technical Journal, Vol. 18, Oct., 1939
- 4) T. Nakai : Proc. Res. Inst. Atm., Nagoya Univ., 6, 22, 1959
- 5) T. Nakai : Proc. Res. Inst. Atm., Nagoya Univ., 5, 30, 1958